# Cronfa - Swansea University Open Access Repository

_____

This is an author produced version of a paper published in:
_Applied Thermal Engineering_

_____

Cronfa URL for this paper:

http://cronfa.swan.ac.uk/Record/cronfa43791

_____

**Paper:**

Sutton, R., Jewell, E., Searle, J. & Elvins, J. (2018). Discharge performance of blended salt in matrix materials for low enthalpy thermochemical storage. _Applied Thermal Engineering_

http://dx.doi.org/10.1016/j.applthermaleng.2018.09.052

_____

# Accepted Manuscript

Discharge performance of blended salt in matrix materials for low enthalpy thermochemical storage

R. Sutton, E. Jewell, J. Searle, J. Elvins

Please cite this article as: R. Sutton, E. Jewell, J. Searle, J. Elvins, Discharge performance of blended salt in matrix materials for low enthalpy thermochemical storage, *Applied Thermal Engineering* (2018), doi: https://doi.org/10.1016/j.applthermaleng.2018.09.052

# Discharge performance of blended salt in matrix materials for low enthalpy thermochemical storage

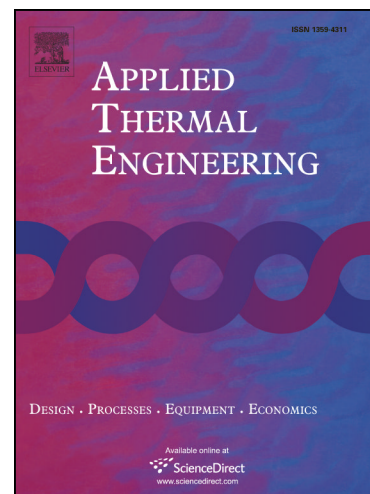R. Sutton[1], E. Jewell[1], J. Searle[1] and J. Elvins[1]

Corresponding author : Dr Eifion Jewell, e.jewell@swansea.ac.uk

1- Swansea University, College of Engineering, Bay Campus, Fabian Way. Crymlyn Burrows, Swansea, SA1 8EN, 437543@swansea.ac.uk, e.jewell@swansea.ac.uk

**Abstract**

A novel study is undertaken on low cost thermochemical storage which utilizes temperatures which are compatible with low grade renewable energy capture. The discharge performance of thermochemical storage matrix materials is assessed using a custom developed experimental apparatus which provides a means of comparing materials under scaled reactor conditions. The basic performance of three salts ($CaCl_2$, $LiNO_3$ and $MgSO_4$) was investigated and their subsequent performance using layering and blending techniques established that the performance could be increased by up to 24% through the correct choice of mixing technique. Layering the $CaCl_2$ on the $LiNO_3$ provided the most efficient thermal release strategy and yielded a thermal storage density of 0.2 $GJ/m^3$. The research also uniquely highlights the important finding that incorrect mixing of the materials can lead to a significant reduction in efficiency with freely mixed $CaCl_2$ and $LiNO_3$ possessing a storage capacity of less than 0.01 $GJ/m^3$ as a result of chemical interactions between the deliquesced materials in close proximity. The paper has impact for the design and control of thermochemical storage systems as it clearly identifies how performance can be improved or degraded by the choice and the structuring of the materials.

## 1. Introduction

Thermochemical storage materials provide an efficient means whereby excess thermal energy can be harvested and utilized at a subsequent time period when there is a demand and is the source of increasing research and development interest,(1–5). It has the potential to provide higher storage densities than sensible or phase change storage and can be tailored to suit the heat source available. In addition, thermochemical storage systems do not suffer from self discharge issues related to directly storing thermal energy(6,7). For the built environment, one such heat source is a transpired solar collector (TSC) which absorbs solar radiation and causes an uplift in the air that is in contact with the absorber surface. This warm air is drawn through a perforated skin into a plenum chamber and is available for further distribution or storage (8). In a northern European climate this system is capable of providing air at a temperature of up to 80 °C (9), which although considered "low grade"

has the potential to be used as an energy source in a building thermal storage system. The principle of operation of such a system is shown in Figure 1. During dry warm periods (Figure 1a), the hot air produced by the TSC can be used to chemically change the storage material and this air can then be safely discharged to the exterior of the building. During colder periods, Figure 1b, the cold air can be elevated in temperature by chemical reactions in the thermochemical storage and supplied directly to the building or as input air with a temperature uplift to a conventional air heating system.



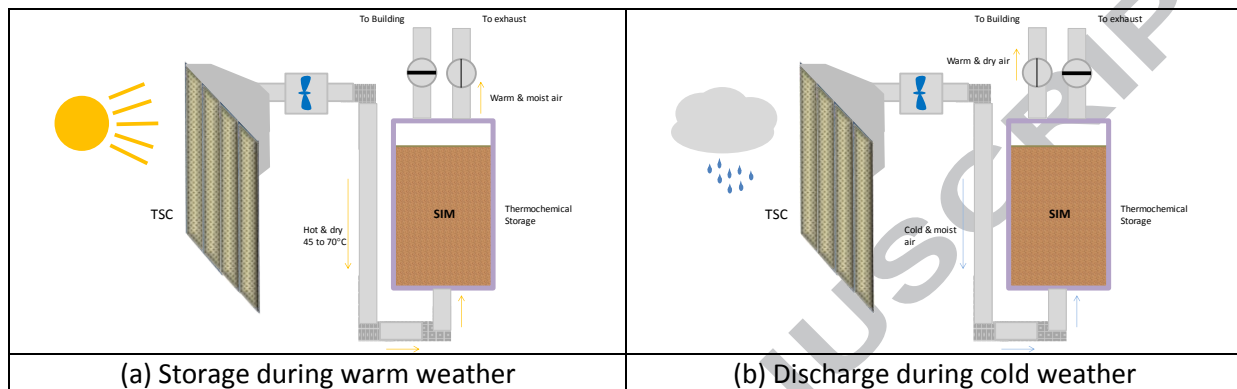| (a) Storage during warm weather | (b) Discharge during cold weather |

Figure 1 : Simplified schematic of charge and discharge stages of salt in matrix (SIM) thermochemical cycle using a transpired solar collector (TSC) for building thermal storage and heating.

A potentially low cost and high storage capacity thermochemical storage material is a salt in matrix (SIM) where the enthalpy of hydration of a salt is used to store energy (10) within an inert matrix which provides a physical scaffold upon which the salt crystals form(11). This matrix provides the large surface area (and hence aids sorption), it also serves to provide a protective structure and can mitigate some of the detrimental effects of deliquescence of the salt during the hydration phase, (12). Numerous salts provide a means of thermochemical storage by hydration (13,14) with the primary factor in determining suitability being the compatibility of the temperatures available from the heat source. A salt which has received a significant amount of attention is Calcium Chloride ($CaCl_2$) which with its many hydration states across a broad temperature range, coupled with its low cost makes it an attractive proposition (15–18). It has also been shown to possess excellent reversibility for multiple charge / discharge cycles (19). Other salts which have been studied include $LiNO_3$(20), $MgSO_4$(21,22), LiBr(23,24), $MgCl_2$ (25), $AlSO_4$ (25), $SrBr_2$(26) and $CuSO_4$ (27).

The ideal SIM provides maximum storage energy density, an even thermal temperature output throughout the discharge process, discharges when supplied with moist air and discharges completely without long term detrimental effect on any subsequent recharge. As each salt has its own characteristics in terms of hydration / dehydration temperature range, hydration / dehydration rate, solubility, corrosive properties and cost there is merit in forming composite / blended salts which balance each salt's properties with the requirements. Composite salts have also been blended to provide a wider operating temperature range and broaden the charge /discharge envelope. (23,28,29). Composite salts can be manufactured and used in a number of ways. Salts can be mixed in solution prior to impregnation into the host matrix or each salt can be impregnated into the matrix individually and either assembled in layers or mixed randomly in the reactor. When $MgCl_2$ was blended with $MgSO_4$ there was an increase in storage capacity, but this required a higher charging temperature of 130 $^{o}$C(30). A blend of pure CaCl2 / MgCl2 was found to have improved kinetic performance and cyclic ability(31), but this study considered small volumes of salt (around 2g) within an idealised environment of analytical laboratory equipment with no host matrix.

Previous work by the authors have highlighted that the performance in bulk (>12 mm of thickness), differs considerably from the performance under laboratory analytical conditions, (32). This work sets out to examine the performance of some of these composite SIM materials when used in a system at a scale more suited to interseasonal heat storage system.

Potential host matrices are selected primarily on their ability to disperse the salt, prevent deliquescence during hydration, possess a high internal surface area on which to disperse the salt, be highly porous (to both gas and liquid phases), lightweight, durable, inert and be of relatively low cost. Casey et al (33,34) completed a relative comprehensive review of various potential host matrices including silica gel, vermiculite (35), activated carbon and zeolite 13X impregnated with a range of inorganic salts. Casey (33) suggests that the silica gel and zeolite 13 X matrices suffered damage to the internal pore network during synthesis. The study also concluded that following impregnation with the salt a reduction in mesopore volume occurs with non-vermiculite matrices, reducing accessibility to moisture and that the vermiculite suffered no such performance degradation.

Much of the work in the literature has been focussed on the fundamental thermodynamic properties of the storage materials through analytical analysis, with venturing into the application of the technology being less frequent. Previous scale studies are well summarised in (2) who identifies that that reactor efficiency is governed by the interaction between the materials, reactor design and operating conditions. Where reported, these have dealt with a fixed mono salt (26,36) with no consideration of mixing to improve performance.

What the literature has highlighted is that there has been considerable effort on the understanding of chemical and thermodynamic characteristics of salt / SIM during hydration and de-hydration process as mono and mixed salts, but only within a small volume under analytical conditions. The scope of the literature reduces when a larger volume of mixed SIM materials are considered, particularly for the temperature range which is compatible with a relatively low grade renewable energy source such as a TSC. Thus, the aim of the study was to examine the interactions between common SIMs and understand, how through the choice and structure of the materials, their combined performance can be enhanced or degraded. This provides further insight into the mechanisms of hydration and also provides design and operational guidelines for applied thermal engineers in the field of reactor design and operation.

## 2. Materials and methods

The 80 °C maximum temperature expected from a TSC limits the choice of suitable salts and therefore $CaCl_2$, $LiNO_3$ and $MgSO_4$ were selected for the present study as their change in hydration levels are within the operational window of the energy source available, (37). Salts were sourced at 99.9% purity from Sigma Aldrich. Salts were impregnated into the vermiculite using fully saturated solutions for each salt. The internal volume of the matrix was measured using a liquid volume method. A mass of matrix was added to an excess volume of water in a suitable container which was placed under a vacuum to remove the air from the internal pores, replacing the evacuated air with solution. Further details of the material manufacture and characterisation are available(32).

The thermal discharge response of each SIM material was evaluated by placing each material into a cylindrical vertically aligned reactor with a diameter 5.5 cm and volume of 700 cm$^3$ with air entering the reactor at the base, as outlined in Figure 2. During the discharge (hydration) portion of the cycle (replicating Figure 1 b) controlled humidity air was used and the temperature and humidity were monitored prior to entrance and exit of the reactor as well as at 3 points along the reactor path.
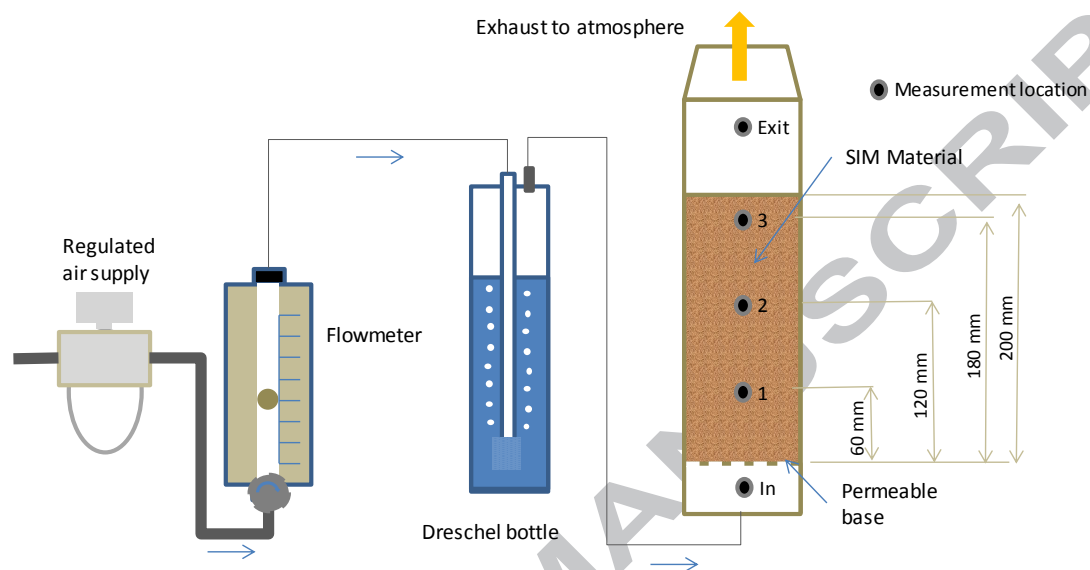


Figure 2: Schematic of the experimental apparatus developed to investigate parameters representative of a typical thermal storage system.

The reactor was filled with 600 cm$^3$ of material leaving a headspace of 100 cm$^3$. Dry air was supplied from a compressed air source and subsequently passed through Dreschel bottles to provide the reactor with air at a constant 19 °C and 12.9 g $H_2O$/cm$^3$ for the $CaCl_2$ and $LiNO_3$ SIM materials and 15.5 g $H_2O$/cm$^3$ for the $MgSO_4$ material as prior evaluations had highlighted limited reactivity at lower water vapour concentrations[38]. These temperature and water vapour concentration level were chosen as it provides sufficient moisture at a rate which provides a measureable change in temperature over a practical experimental period, [32], it represents a water vapour concentrations which is comparable to trends observed UK Autumn / Winter levels[39] and it could be provided consistently in the laboratory over the entire measurement period [32]. Temperature and humidity were monitored using type K thermocouples and a TE-HPP805C031 RH sensor at the locations identified in Figure 2. Prior to discharge analysis, materials were charged using an oven set to 120 °C for 48 hours to ensure that the entire sample was all at its lowest hydration state, i.e. $CaCL_2.2H_2O$, $LiNO_3.1H_2O$ and $MgSO_4.1H_2O$.

## 3. Results

Prior to assessment of the composite matrices, it is important to examine each material in isolation so as to identify the merit of each SIM, to act as a reference against which combinations could be compared and to identify likely successful combinations. An ideal SIM / SIM combination would provide a maximum temperature uplift consistently during the discharge period.

### 3.1 Single SIM operation

The response of each individual SIM identifies the behaviour of each material and acts as a baseline against which their combined performance can be compared. The relative rate of hydration and thermal response of each salt in the vermiculite SIM differs considerably, as shown in Figure 3. For each SIM, thermal and water vapour concentrations are shown at the base and mid reactor with key characteristics summarized in Table 1 and 2. In all instances peak temperatures are generated in the first hour of exposure to the moist air at the base of the reactor. During the period of energy liberation, the local moisture level is depressed compared to the input air indicating an interaction between the SIM and moisture. There is further reduction in moisture concentration as one proceeds through the reactor as the hydration reactions proceed. These temperature profiles are similar in form to those predicted by reactor numerical models, although the absolute magnitude of the temperature rise is lower (40).

Table 1 : Temperature rises in the reactor at each position relative to the air entry point for each single SIM material ($^o$C). "Average" denotes the mean temperature uplift at the position over the 40 hour experimental period while "Max" denotes the peak temperature uplift.

| Position → | 1 | | 2 | | 3 | | Exit | |
|---|---|---|---|---|---|---|---|---|
| Temperature °C | Average | Max | Average | Max | Average | Max | Average | Max |
| V-CaCl$_2$ | 8.8 | 25.3 | 11.2 | 18.9 | 9.5 | 13.6 | 6.0 | 9.7 |
| V -LiNO$_3$ | 6.1 | 16.6 | 6.8 | 21.4 | 5.5 | 20.3 | 2.8 | 8.7 |
| V-MgSO$_4$ | 3.7 | 15.4 | 2.5 | 10.0 | 1.2 | 6.4 | 0.3 | 2.9 |

Table 2 : Reactor exit temperature uplift (°C) of each SIM in the reactor in single SIM mode

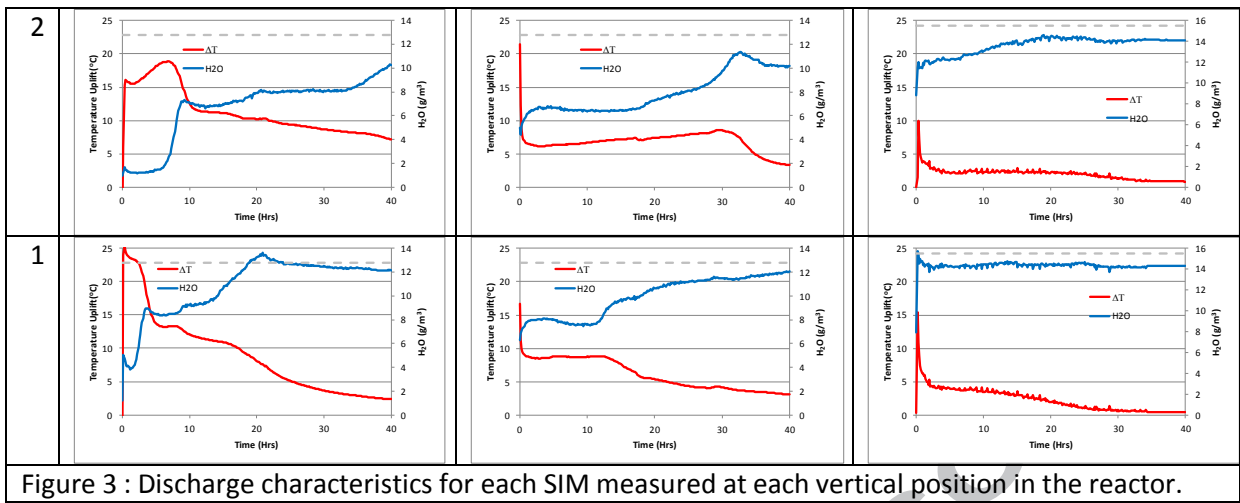| ΔT (°C) | V-CaCl$_2$ | V-LiNO$_3$ | V-MgSO$_4$ |
|---|---|---|---|
| @1 hr | 4.4 | 2.6 | 2 |
| @10 hrs | 6.4 | 2.3 | 0.1 |
| @20 hrs | 9.6 | 2.7 | 0.1 |
| @30 hrs | 5.0 | 3.3 | 0.6 |
| @40 hrs | 4.0 | 3.7 | 0.4 |
| Mean | 5.9 | 2.9 | 0.6 |
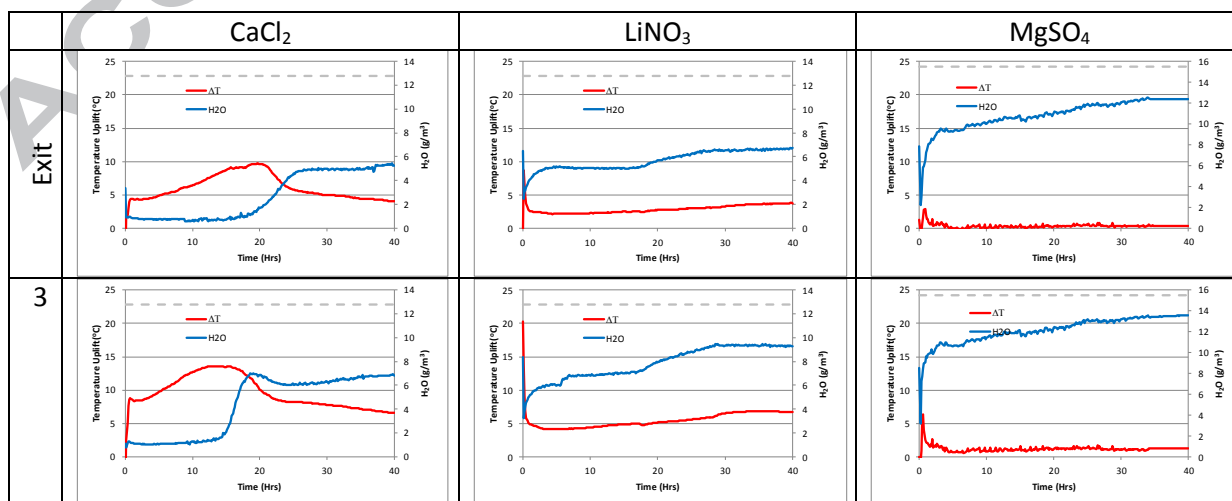
Figure 3 : Discharge characteristics for each SIM measured at each vertical position in the reactor.

The proposed mechanism for hydration and energy release from the SIM materials can be explained by the reactor temperature, humidity and absorbed moisture profiles in each reactor section, Figure 4. The absorption profile is calculated by examining the change in moisture content between the inlet of each section and that which exits each section, the difference being that which has 'reacted' via hydration, adsorption or deliquescence in this section. From the mass of salt and salt characteristics within each section the accumulated moisture as a percentage of stoichiometric quantity required for exothermic hydration (100%) can be obtained. Excessive accumulation (>100%) results in deliquescence while accumulation levels below 100% indicate poor utilization of the available moisture. Through examination of the moisture availability through the reactor it is possible to explain the thermodynamic response of the reactor with each material.
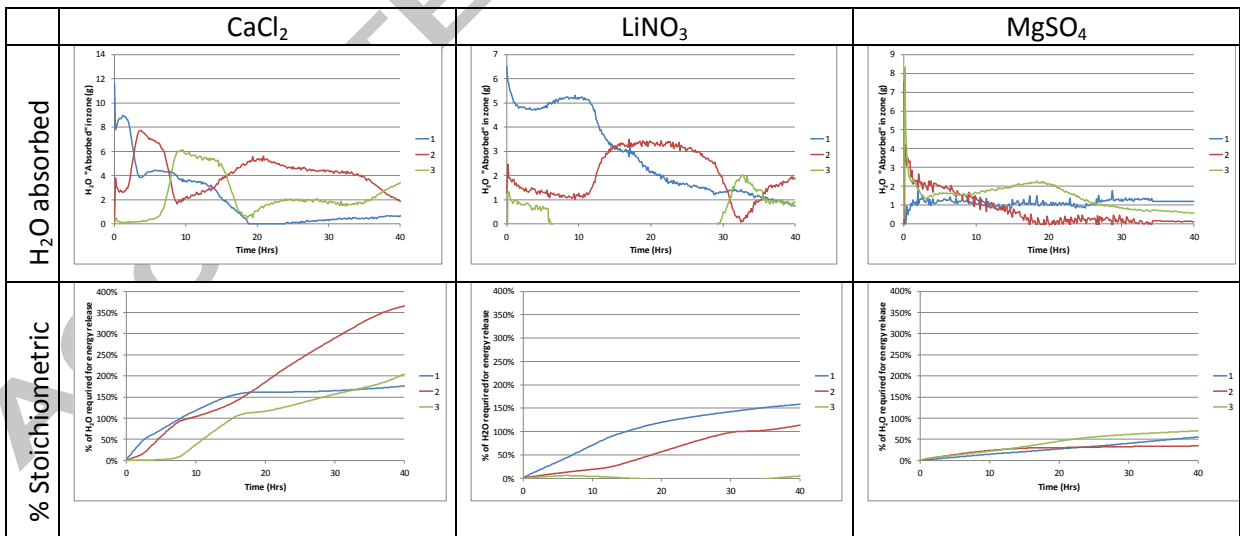


Figure 4 : Accumulated moisture for each SIM measured at each vertical position in the reactor.

The initial peak temperature rise is associated with the hydration reaction on the SIM surface. This reaction liberates energy and depresses the local humidity as moisture is drawn from the air. Once the surface salt has reacted, the reaction rate reduces (resulting in lower temperatures) as the water vapour must pass into the inner layers of the SIM and there is a subsequent small increase in the local humidity level as water is drawn from the air at a slower rate. As the salt reactant within the

SIM is used, then the local vapour is no longer reduced and vapour is able to pass to the next stage and the rate of energy liberation (and hence local temperature) reduces.

The $CaCl_2$ SIM produces a peak temperature rise of 25 °C at the base of the reactor and this is maintained for approximately 4 hours before reducing gradually over the remaining 36 hours of the test period. Further along the reactor path, similar trends are observed except that the absolute temperature increases are reduced and there is a time delay in the point at which the maximum temperature is reached. This reflects a sorption wave related to the moisture availability further along the reactor path. The low exit moisture level with the $CaCl_2$ is associated with the excess deliquescence of the $CaCl_2$ whereby moisture is drawn from the air, even when it is unfavourable to the release of energy (19,32,41). The relationship between the moisture absorption (Figure 4) and thermal response (Figure 3) is clearly evident with the $CaCl_2$ where the local temperature maximums coincide with the exothermic hydration absorption while thermal response is lower where excessive moisture is absorbed through deliquescence. This deliquescence is evident in Figure 4 where two thirds of the material absorbs an excess of moisture within a 5 hour period with the central section absorbing around 350% of the required moisture over the 40 hour period. This finding has an impact on the maximum permissible moisture / SIM path length which can be used with such a reactor. It also highlights the importance and impact of control and monitoring philosophies for any scaled reactor. Poor engineering design or poor control of the extent or distribution of hydration via moisture delivery can significantly impact on the evolved thermal energy that is available and thus reduce the overall efficiency and viability of a scaled thermochemical storage unit.

The $LiNO_3$ provides the most consistent temperature uplift at the exit, averaging a temperature uplift of between 3 and 4 °C. Peak temperatures over 10 °C are experienced for around 20 hours of operation in the reactor base and this reduces to around 5°C over the experimental period. The $MgSO_4$ SIM temperature profile is characterised by a rapidly dissipating peak at the reactor base and a gradual temperature rise of around 1 °C. The moisture level increases rapidly, nearing the inlet moisture level at the base indicating that there is minimal interaction between the SIM and the water vapour. Further along the reactor the moisture level of the air in the $MgSO_4$ SIM lowers only by a small amount indicating that some SIM / water vapour interaction occurs, although the net thermal result is negligible. This can be attributed to the lower moisture uptake rate illustrated in Figure 4. The poor temperature uplift performance of the $MgSO_4$ has been observed previously (22,25,36) and is a result of the relative inactivity at low humidity levels, (42). Energy is liberated near the reactor inlet, which reduces the moisture levels for the air passing through the remainder of the reactor, limiting the availability of moisture and hence energy liberation in the latter reactor sections. The energy liberated in the early stages of the chamber is then absorbed by the thermal mass of the unreacted material with a subsequent reduction in exit thermal uplift.

In each case the air exit temperature is lower than that achieved in the reactor core and is a result of the energy liberated in the reactor being absorbed by the inactive mass in the reactor. Some of the energy is absorbed by the SIM material itself, the air temperature increase is diluted by the unreacted air passing around the SIM and a portion is also absorbed by the reactor body itself, in areas where significant over saturation of the SIM material occurs, the increased thermal mass of the water will also reduce the overall energy liberation at the exit of the vessel. Each SIM therefore has its advantages and disadvantages in terms of discharge performance, Table 3, and this dictates likely combinations which may have superior performance.

Table 3 : Summary of performance of each individual SIM material

| SIM material | Advantages | Disadvantages |
|---|---|---|
| $CaCl_2$ | • High relative temperature uplift<br>• Good thermal release in low moisture levels<br>• Low cost | • High tendency for deliquescence |
| $LiNO_3$ | • Single hydration energy release step. | • Significantly higher costs<br>• Limited energy density. |
| $MgSO_4$ | • Largest potential energy storage<br>• Uniform moisture absorption through reactor<br>• Minimal agglomeration<br>• Reduced tendency for deliquescence | • Poor response at low humidity levels<br>• Low peak temperatures<br>• Rapid drop off from initial peak |

### 3.3 Layered SIM operation

In order to improve the thermal response of the individual SIM materials, the materials were combined in number of ways using a layering approach. The tendency of the $CaCl_2$ SIM to deliquesce dictates that it would operate most efficiently when subjected to lower humidity air, allowing reaction and energy liberation while minimizing excess interaction with the moisture. It was subsequently placed in the upper region of the reactor.

The response of a 2 layered system with $CaCl_2$ as the upper SIM illustrates that it is possible to provide an extended period of temperature uplift utilising a $LiNO_3$ / $CaCl_2$ layered approach, Figure 5 (a). There is an initial reaction between the $LiNO_3$ and the moist air which liberates energy at the lower part of the reactor for the first 15 hours with a reduction in the air moisture level. This reduced moisture air subsequently passes into the upper portion of the reactor where the $CaCl_2$ scavenges the remainder of the moisture and liberates energy as a result. As the $LiNO_3$ becomes fully hydrated, the moist air passes through the lower stages unhindered allowing the $CaCl_2$ to react and liberate further energy before eventually becoming fully hydrated with a reduction in temperature as the $CaCl_2$ SIM begins to deliquesce. The net result is a mean exit temperature uplift of 7.6 °C over a 40 hour period, Table 4. This is around a 24% improvement over the single operation with $CalCl_2$ SIM only, Table 2. No deliquescence was observed in the $CaCL_2$ SIM during its operation above the $LiNO_3$ SIM, thus the layering has the added benefit of eliminating this detrimental characteristic. Layering of the $CaCl_2$ SIM on top of the $MgSO_4$ SIM does not result in any improvement in the performance in the temperature lift from the reactor. As with the single operation, the energy liberated from $MgSO_4$ is minimal at these humidity levels. The relative inactivity of the MgSO4 in the lower portion of the reactor means that the $CaCl_2$ SIM is exposed to higher moisture levels and therefore tends to deliquesce resulting in lower exit moisture levels and temperature uplift, Figure 4(b).
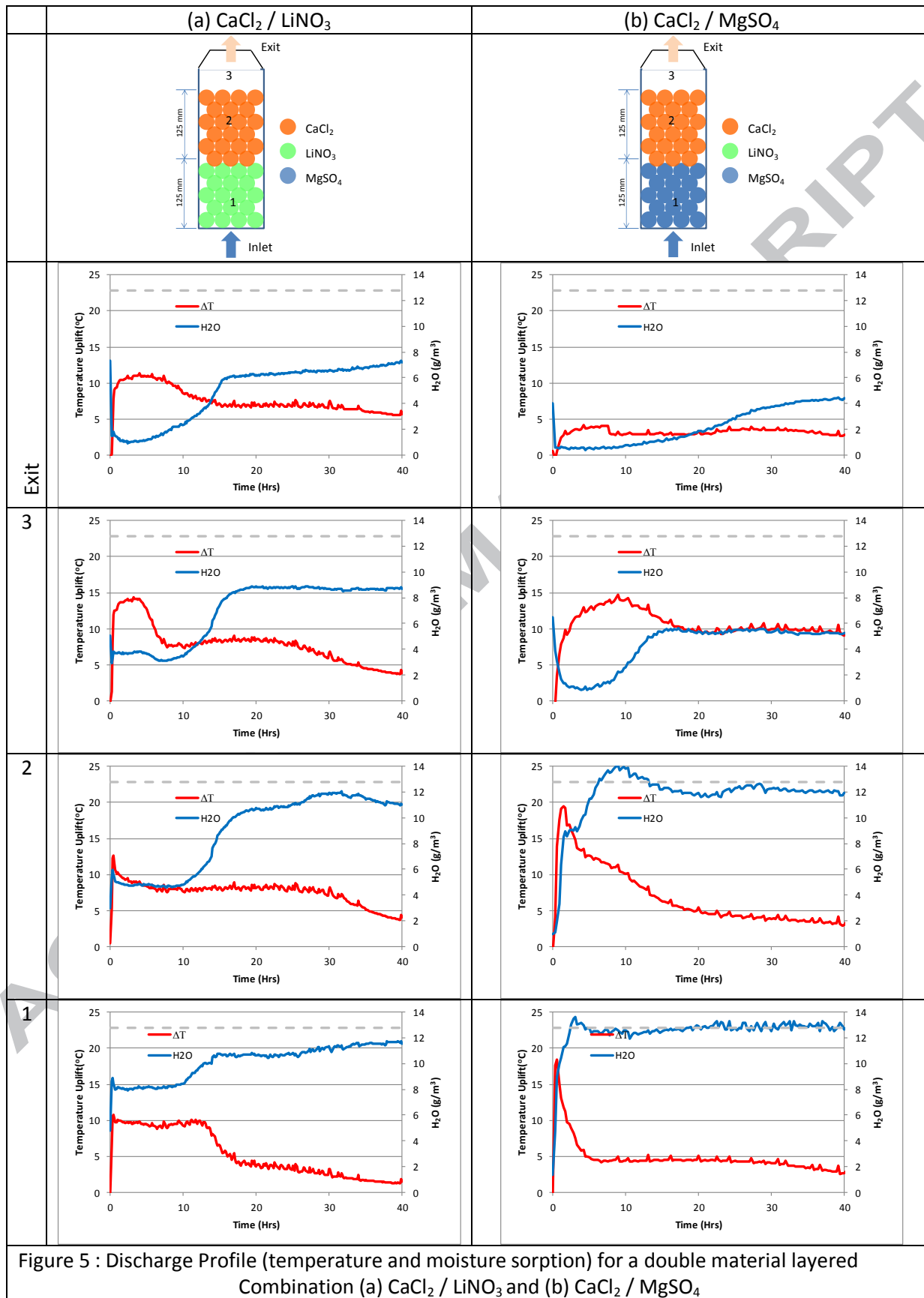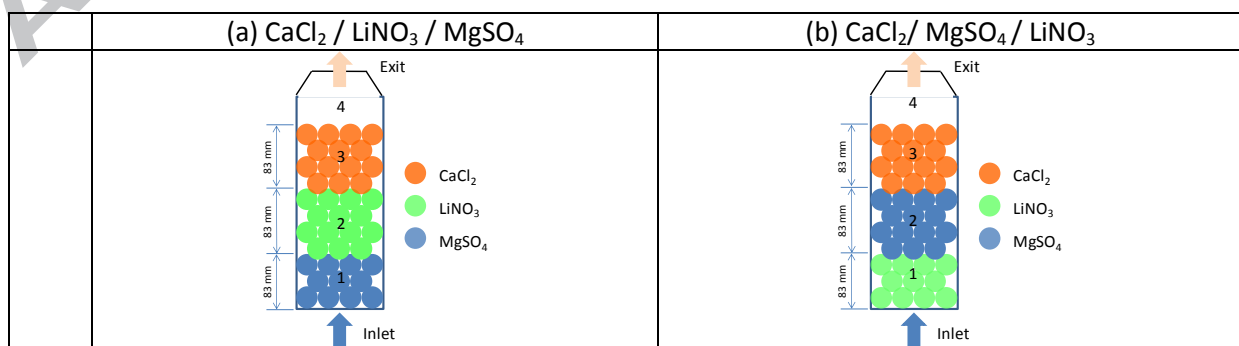
Figure 5 : Discharge Profile (temperature and moisture sorption) for a double material layered Combination (a) CaCl$_2$ / LiNO$_3$ and (b) CaCl$_2$ / MgSO$_4$

In order to further examine the benefit of material layering within the reactor, three-layer systems were also investigated. Each layer constituted 1/3 of the reactor length with the $CaCl_2$ SIM consistently being the upper SIM material as this ensured that the material most likely to deliquesce was not subjected to the highest moisture levels. Temperature and humidity were monitored within each material in the reactor.  The thermal characteristics observed in a triple layered system are in line with thermal characteristics of the individual materials.

In all instances the reactor exit moisture level is depressed compared to the input moisture level throughout the test period, indicating there remains an interaction between the water vapour in the air and the SIM materials, Figure 6. In both layering regimes, the temperature / moisture profile near the inlet is similar to the temperature / moisture profile when the same single salt in used in this region indicating that the local impact of the downstream material is minimal. With the $MgSO_4$ in the base, the local temperature uplift in the reactor core is modest (around 5 °C) but consistent as the relatively slow reaction between the $MgSO_4$ and moisture occurs. The lower moisture level relative to the input air in this section provides additional evidence of the hydration reaction. There is little evidence of reaction between the $LiNO_3$ and the moist air in the central layer of the reactor as the moisture level remains similar to the base region and there is a reduction in temperature as the thermal mass of the SIM in this region acts as a sink.

Although the difference observed in the exit moisture profile between the two layering options is relatively small, the temperature uplift is greater when $LiNO_3$ is placed at the base. With the $LiNO_3$ in the base of the reactor, a characteristic spike in temperature uplift is seen at the base of the reactor, Figure 6(b), although the peak temperature uplift is relatively short. This suggests an initial reaction of the free salt on the SIM surface with a continued reduced rate of reaction with the $LiNO_3$ within the SIM. This reduced reaction rate results in a subsequent increase in local free moisture level and allows passage of the high moisture air into the MgSO4 where the moisture is of a sufficient level to provide a minimal reaction with the relatively inactive $MgSO_4$.

The overall thermal uplift for the triple layered system is poorer than the double layered system and the sensitivity to the layering structure highlights the complexity of the salt / moisture reaction kinetics and their subsequent impact of reactor efficiency. The choice of SIM and its subsequent reaction with the moisture has a direct impact on the likely reaction in those regions further downstream.
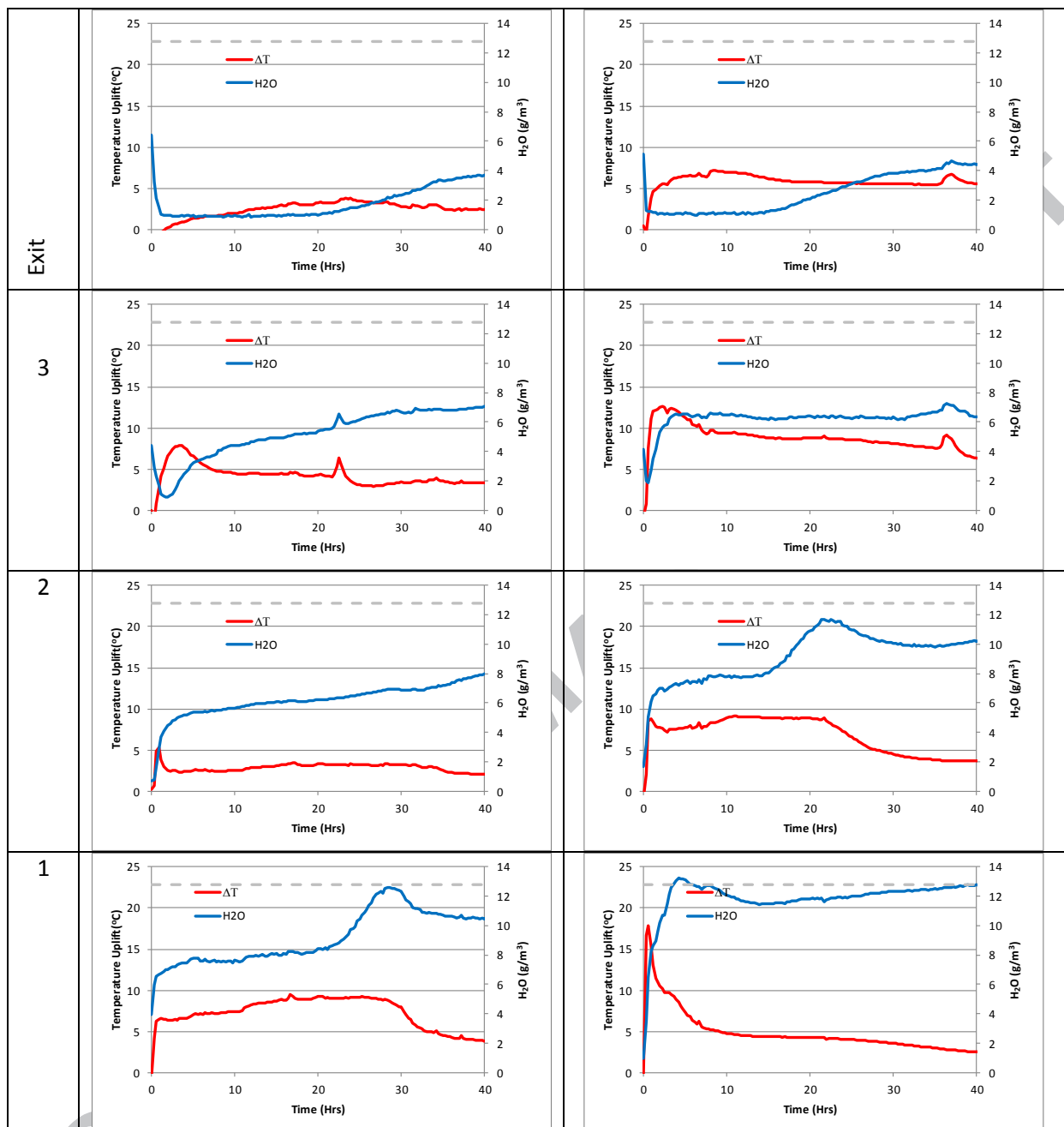
| (a) CaCl$_2$ / LiNO$_3$ / MgSO$_4$ | (b) CaCl$_2$/ MgSO$_4$ / LiNO$_3$ |
| --- | --- |
|  |  |

Figure 6 : Discharge Profile (temperature and moisture sorption) for a three material layered Combination (a) $CaCl_2$ / $LiNO_3$ / $MgSO_4$ and (b) $CaCl_2$/ $MgSO_4$ / $LiNO_3$

Table 4 : Reactor exit thermal temperature uplift (°C) of each SIM in the reactor with layered SIM

| | $CaCl_2$ / $LiNO_3$ | $CaCl_2$ / $MgSO_4$ | $CaCl_2$ / $LiNO_3$ / $MgSO_4$ | $CaCl_2$ / $MgSO_4$/ $LiNO_3$ |
|---|---|---|---|---|
| $\Delta T$@1hrs °C | 9.9 | 2.4 | 0.0 | 4.6 |
| $\Delta T$@10hrs °C | 8.5 | 2.9 | 2.0 | 7.0 |
| $\Delta T$@20hrs °C | 6.9 | 3.4 | 3.3 | 5.8 |
| $\Delta T$@30hrs °C | 7.2 | 3.4 | 2.8 | 5.6 |
| $\Delta T$@40hrs °C | 5.7 | 2.7 | 2.4 | 5.6 |
| Mean | 7.6 | 3.0 | 2.1 | 5.7 |

### 3.4 Blended SIM operation

The performance envelope of the SIMs when blended in equal mass proportions was also examined to determine their composite performance, Figure 7 and Table 5. Blending the materials gave no discernible improvement in the performance.

When $MgSO_4$ and $LiNO_3$ are blended, Figure 7(a), the temperature profile follows a similar pattern to the layered counterpart, although the magnitude of temperature uplift is lower. This is associated with the lower degree of reaction between the SIM and water vapour as shown by the higher exit moisture level at the exit throughout the discharge period. Blended $CaCl_2$ and $MgSO_4$ SIM materials produce a similar output profile to the solo $CaCl_2$ profile, although the overall temperature uplift is reduced, Figure 7(b).This is evidenced by the higher exit moisture level when compared to the $CaCl_2$ on its own, Figure 3, indicating a lower reaction and deliquescence level within the reactor. When $CaCl_2$ and $LiNO_3$ were blended there was a substantial reduction in reactor performance Figure 7(c) which is attributed to the excess deliquescence of the $CaCl_2$ within the blend which is both thermodynamically unfavourable and adds additional mass as a thermal sink. The initial thermal uplift induced by the salt hydration is seen as a small temperature uplift at the exit (around 1.5 °C), but ceases at around 16 hours. As the exit moisture level remains more or less constant at a low level throughout the experimental period it is postulated that the blending induces greater moisture capture within the reactor which leads to a reduction in the core temperature as an excess of water is deposited increasing its thermal mass. This excess deposition of water in the core also starves the material further up the reaction chamber of the moisture required for the release thermal energy. A similar scenario is observed when all SIM materials are blended in equal proportion, Figure 7(d).
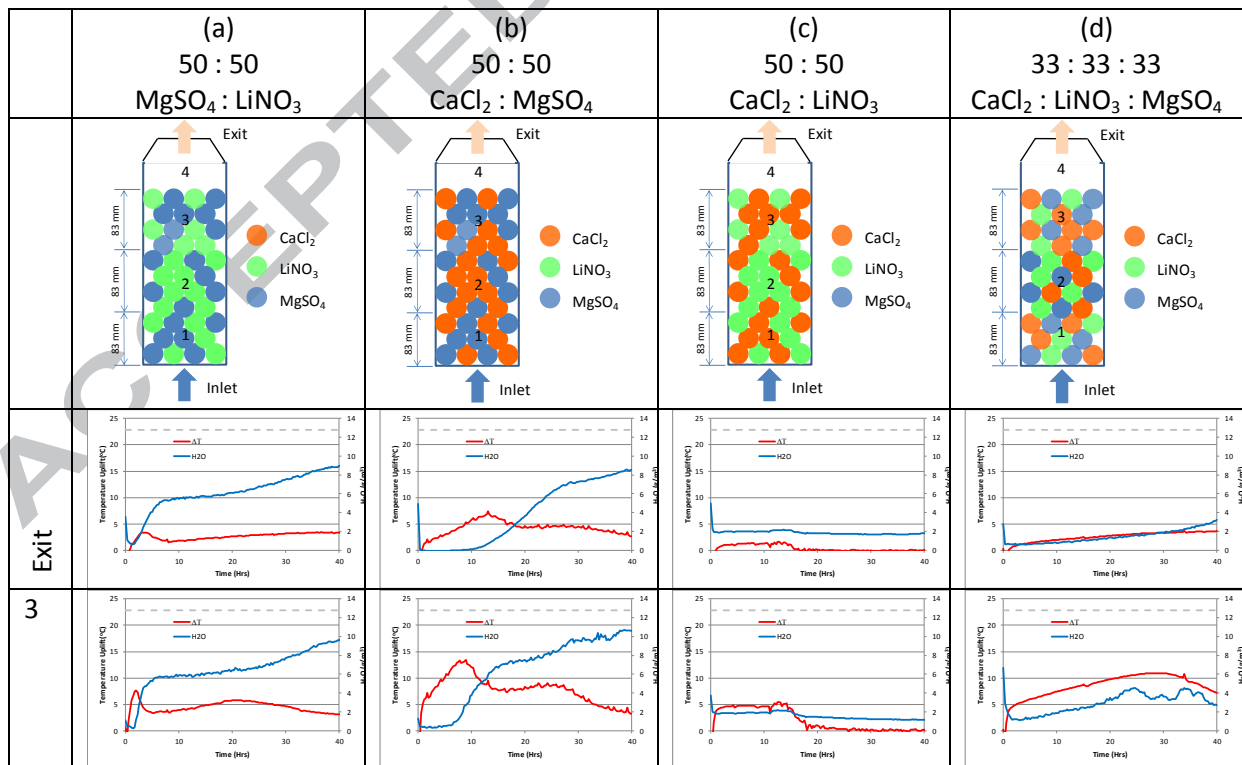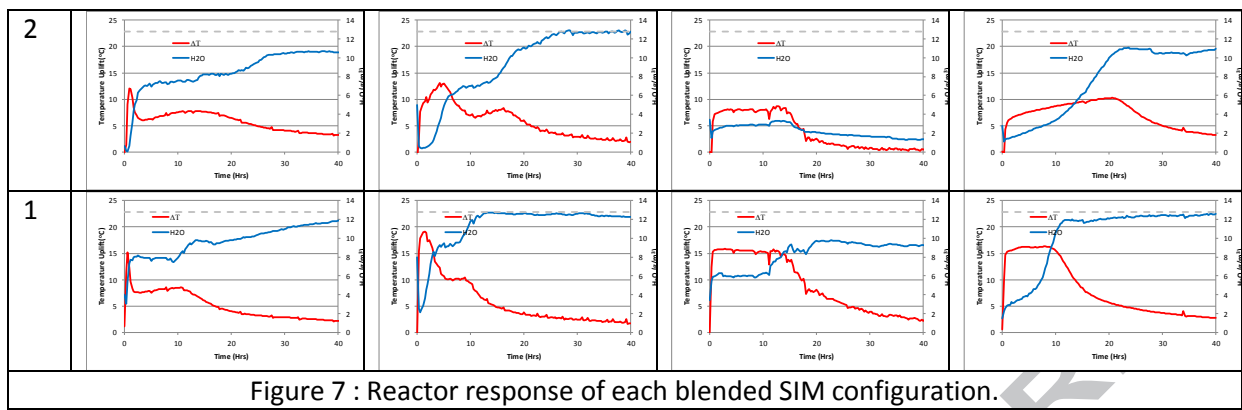
Figure 7 : Reactor response of each blended SIM configuration.

Table 5 : Reactor exit thermal temperature uplift (°C) of each SIM in the reactor when blended

|  | LiNO$_3$/MgSO$_4$ | CaCl$_2$/MgSO$_4$ | CaCl$_2$/ LiNO$_3$ | CaCl$_2$/MgSO$_4$/ LiNO$_3$ |
|---|---|---|---|---|
| ΔT@1hrs °C | 1.0 | 1.3 | 0.3 | 0.2 |
| ΔT@10hrs °C | 1.8 | 5.8 | 1.3 | 2.0 |
| ΔT@20hrs °C | 2.6 | 4.6 | 0.1 | 2.8 |
| ΔT@30hrs °C | 3.2 | 4.5 | 0.0 | 3.3 |
| ΔT@40hrs °C | 3.3 | 2.6 | 0.0 | 3.6 |
| Mean | 2.4 | 3.8 | 0.4 | 2.4 |

The relative performance of the SIM mixing / layering shows that average and maximum exit temperature uplift can be increased by around 15% through layering SIM materials which have a high tendency to react / absorb water vapour within the later stages of the chamber, Figure 8. This prevents their water scavenging behaviour leading to poor salt utilization in further on in the chamber. However, if the reactivity between the upstream SIM salt is too low, e.g. MgSO$_4$, then there is no benefit of layering the SIMs as the low reactivity material acts as a thermal sink on the reactive material, reducing the overall air temperature uplift.



(a) Reactor core
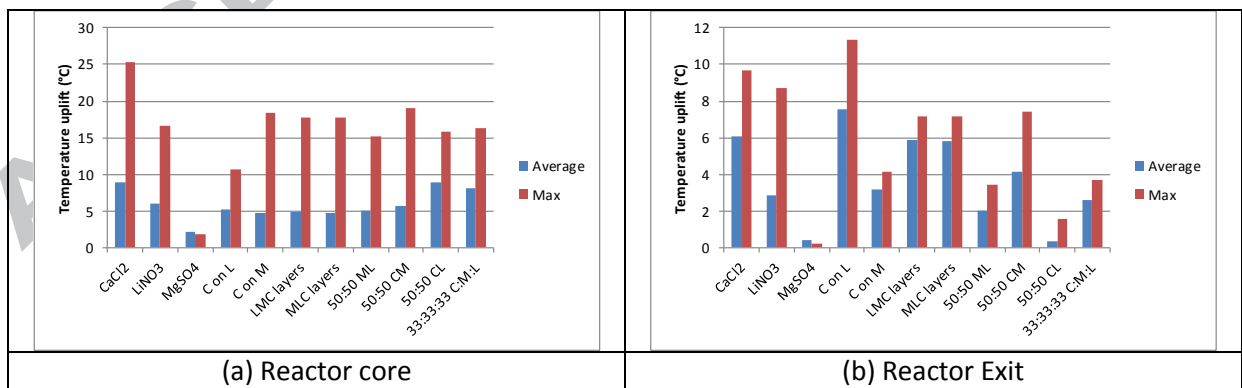
(b) Reactor Exit

Figure 8 : Maximum and average temperature uplift experienced by the air in (a) Reactor core and (b) Reactor exit. (Notation: C – CaCl$_2$, L –LiNO$_3$, M – MgSO$_4$).

From the mass and type of salt in the reactor it is possible to calculate the total energy stored if the salt undergoes hydration from its hydrated state at 80 °C to its maximum hydrated state (2 to 7 CaCl$_2$, 1 to 3 LiNO$_3$ and 1 to 4 MgSO$_4$). Integration of the thermal response at the reactor exit over

the 40 hour period for the flow rate specified and including the thermal mass of the reactor allows an evaluation of the reactor efficiency defined as the ratio (as a percentage) of the energy extracted to the air to that which is held stored within the reactor. Layering the $CaCl_2$ on the $LiNO_3$ provides the most efficient release of energy, although the benefit over a single layer $CaCl_2$ is small, Figure 9(a) and this also results in the highest storage density, Figure 9(b). The inclusion of the $MgSO_4$ does not have a positive effect on the performance and cannot be recommended unless there is a way of artificially increasing the humidity.
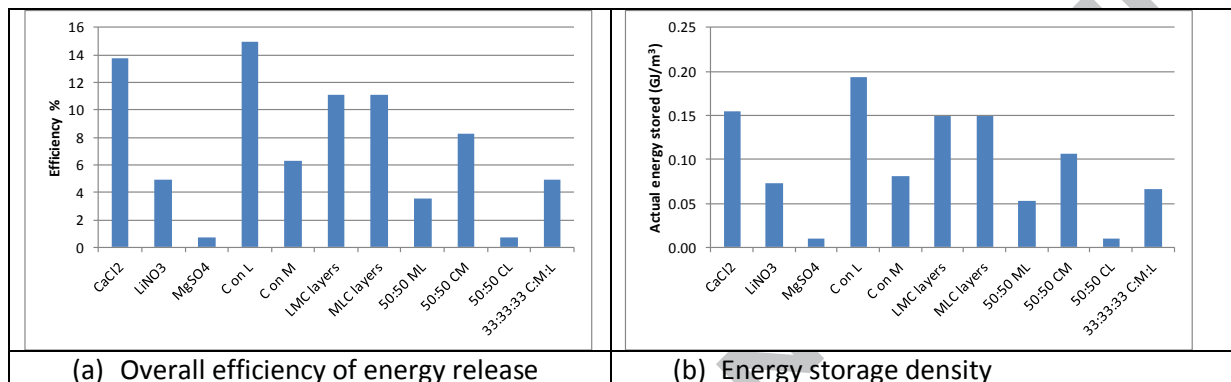


| (a)  Overall efficiency of energy release | (b)  Energy storage density |
|---|---|

Figure 9 : Summary of mixing strategy performance (Notation: C – $CaCl_2$, L –$LiNO_3$, M – $MgSO_4$)

The mechanisms by which reactor efficiency is lowered can be understood by examining the position and extent to which moisture is absorbed in each section of the reactor, Figure 10. In each instance the stoichiometric quantity of moisture required for exothermic hydration (100%) is compared to the change in air moisture through the reactor. In all instances where $CaCl_2$ is used, an excess (>100%) of moisture is absorbed in this section of the reactor which results in a reduction in the temperature uplift. The $MgSO_4$ is continually under-utilized (<100%) and this is reflected in the low thermal response of the SIM.
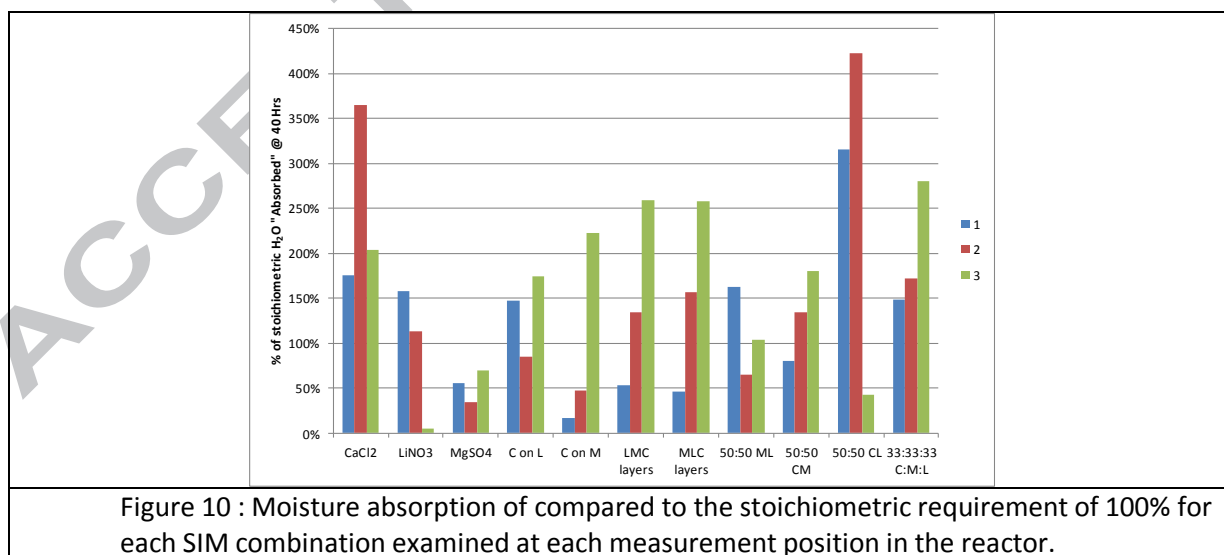


Figure 10 : Moisture absorption of compared to the stoichiometric requirement of 100% for each SIM combination examined at each measurement position in the reactor.

Throughout the investigation, the measured temperature uplifts are relatively modest (7.6 °C for 40 hours) and the efficiency of energy transfer is low (a maximum of 15%), with even the most optimum SIM layering. This represent 0.2 $GJ/m^3$ and equates to 15 $m^3$ of air with a 7 °C uplift from 0.0006 $m^3$ (600 $cm^3$) of material.

## 5. Conclusions

An experimental study on the performance of mixed SIM materials has been carried out in order to assess their capabilities for thermal storage. The thermal response of the materials can be directly linked to the local moisture level and the accumulation of changes in moisture level. The study has identified that there can be a benefit in energy release and subsequent temperature uplift if the appropriate SIM materials are mixed in the reactor. In multi salt systems, the choice and location of the materials governs the effectiveness of the reactor and has a dramatic impact on the performance of the materials. Placing lower reactivity SIM materials close to the inlet of the reactor has a beneficial impact on material utilization and uplift produced by the reactor. Over saturation and subsequent deliquescence of the more reactive salts reduce the performance of the overall chamber in mixed systems if they are placed in areas of highest humidity, this is likely due to the increased thermal mass and dH of solution. Arrangements of the SIMS such that deliquescence is minimised but utilisation is high are beneficial in terms of storage efficiency. The findings have implications for the installation and operation of thermal storage reactors.

## References

1.  Pinel P, Cruickshank CA, Beausoleil-Morrison I, Wills A. A review of available methods for seasonal storage of solar thermal energy in residential applications. Renew Sustain Energy Rev [Internet]. 2011;15(7):3341–59. Available from: http://dx.doi.org/10.1016/j.rser.2011.04.013

2.  Solé A, Martorell I, Cabeza LF. State of the art on gas-solid thermochemical energy storage systems and reactors for building applications. Renew Sustain Energy Rev [Internet]. 2015;47:386–98. Available from: http://dx.doi.org/10.1016/j.rser.2015.03.077

3.  Cot-Gores J, Castell A, Cabeza LF. Thermochemical energy storage and conversion: A-state-of-the-art review of the experimental research under practical conditions. Renew Sustain Energy Rev [Internet]. 2012;16(7):5207–24. Available from: http://dx.doi.org/10.1016/j.rser.2012.04.007

4.  N'Tsoukpoe KE, Liu H, Le Pierr??s N, Luo L. A review on long-term sorption solar energy storage. Renew Sustain Energy Rev. 2009;13(9):2385–96.

5.  Heier J, Bales C, Martin V. Combining thermal energy storage with buildings - A review. Renew Sustain Energy Rev [Internet]. 2015;42:1305–25. Available from: http://dx.doi.org/10.1016/j.rser.2014.11.031

6.  Aydin D, Casey SP, Riffat S. The latest advancements on thermochemical heat storage systems. Renew Sustain Energy Rev [Internet]. 2015;41:356–67. Available from: http://dx.doi.org/10.1016/j.rser.2014.08.054

7.  Eames, Philip; Dennis, Loveday; Victoria, Haines; Romanos P. The Future Role of Thermal Energy Storage in the UK Energy System : An Assessment of the Technical Feasibility and Factors Influencing Adoption Research Report The Future Role of Thermal Energy Storage in the UK Energy System : An assessment of the Techni. Res Rep (UKERC London) [Internet]. 2014; Available from: www.ukerc.ac.uk

8.  Shukla A, Nkwetta DN, Cho YJ, Stevenson V, Jones P. A state of art review on the performance of transpired solar collector. Renew Sustain Energy Rev [Internet]. 2012;16(6):3975–85. Available from: http://www.sciencedirect.com/science/article/pii/S1364032112001232

9. Leon MA, Kumar S. Mathematical modeling and thermal performance analysis of unglazed transpired solar collectors. Sol Energy. 2007;81(1):62–75.

10. Scapino L, Zondag HA, Van Bael J, Diriken J, Rindt CCM. Energy density and storage capacity cost comparison of conceptual solid and liquid sorption seasonal heat storage systems for low-temperature space heating. Renew Sustain Energy Rev [Internet]. 2017;76(March):1314–31. Available from: http://dx.doi.org/10.1016/j.rser.2017.03.101

11. Donkers PAJ, Sögütoglu LC, Huinink HP, Fischer HR, Adan OCG. A review of salt hydrates for seasonal heat storage in domestic applications. Appl Energy [Internet]. 2017;199:45–68. Available from: http://dx.doi.org/10.1016/j.apenergy.2017.04.080

12. De Jong AJ, Trausel F, Finck C, Van Vliet L, Cuypers R. Thermochemical heat storage - System design issues. Energy Procedia [Internet]. 2014;48:309–19. Available from: http://dx.doi.org/10.1016/j.egypro.2014.02.036

13. Trausel F, De Jong AJ, Cuypers R. A review on the properties of salt hydrates for thermochemical storage. Energy Procedia [Internet]. 2014;48:447–52. Available from: http://dx.doi.org/10.1016/j.egypro.2014.02.053

14. Simonova I, Aristov Y. Hydrates. or Storage O. Low Temperature Heat: Selection O. Promising Reactions and Nanotailoring O. Innovative Materials. Int Sci J Altern Energy Ecol [Internet]. 2007;10(210):65–9. Available from: http://isjaee.hydrogen.ru/pdf/pdf/10-07/Simonova_65.pdf

15. N'Tsoukpoe KE, Rammelberg HU, Lele AF, Korhammer K, Watts BA, Schmidt T, et al. A review on the use of calcium chloride in applied thermal engineering. Appl Therm Eng [Internet]. 2015;75:513–31. Available from: http://dx.doi.org/10.1016/j.applthermaleng.2014.09.047

16. Gordeeva L, Grekova A, Krieger T, Aristov Y. Composites "binary salts in porous matrix" for adsorption heat transformation. Appl Therm Eng [Internet]. 2013;50(2):1633–8. Available from: http://dx.doi.org/10.1016/j.applthermaleng.2011.07.040

17. Zeng D, Zhou H, Voigt W. Thermodynamic consistency of solubility and vapor pressure of a binary saturated salt + water system. II. CaCl2 + H2O. Fluid Phase Equilib. 2007;253(1):1–11.

18. Jabbari-Hichri A, Bennici S, Auroux A. Enhancing the heat storage density of silica–alumina by addition of hygroscopic salts (CaCl2, Ba(OH)2, and LiNO3). Sol Energy Mater Sol Cells [Internet]. 2015;140:351–60. Available from: http://dx.doi.org/10.1016/j.solmat.2015.04.032

19. Molenda M, Stengler J, Linder M, Wörner A. Reversible hydration behavior of CaCl2 at high H2O partial pressures for thermochemical energy storage. Thermochim Acta [Internet]. 2013;560:76–81. Available from: http://dx.doi.org/10.1016/j.tca.2013.03.020

20. Shamberger PJ, Reid T. Thermophysical properties of lithium nitrate trihydrate from (253 to 353) K. J Chem Eng Data. 2012;57(5):1404–11.

21. Hongois S, Kuznik F, Stevens P, Roux JJ. Development and characterisation of a new MgSO4-zeolite composite for long-term thermal energy storage. Sol Energy Mater Sol Cells. 2011;95(7):1831–7.

22. van Essen VM, Zondag H a., Gores JC, Bleijendaal LPJ, Bakker M, Schuitema R, et al. Characterization of MgSO4 Hydrate for Thermochemical Seasonal Heat Storage. J Sol Energy Eng. 2009;131(4):041014.

23. Gordeeva LG, Grekova AD, Krieger T a., Aristov YI. Adsorption properties of composite materials (LiCl+LiBr)/silica. Microporous Mesoporous Mater [Internet]. 2009;126(3):262–7. Available from: http://dx.doi.org/10.1016/j.micromeso.2009.06.015

24. N'Tsoukpoe KE, Le Pierr??s N, Luo L. Experimentation of a LiBr-H2O absorption process for long term solar thermal storage. Energy Procedia. 2012;30:331–41.

25. van Essen VM, Cot Gores J, Bleijendaal LPJ, Zondag H a., Schuitema R, Bakker M, et al. Characterization of Salt Hydrates for Compact Seasonal Thermochemical Storage. ASME 2009 3rd Int Conf Energy Sustain Vol 2 [Internet]. 2009;2:825–30. Available from: http://proceedings.asmedigitalcollection.asme.org/proceeding.aspx?articleid=1648078

26. Michel B, Mazet N, Neveu P. Experimental investigation of an innovative thermochemical process operating with a hydrate salt and moist air for thermal storage of solar energy: Global performance. Appl Energy [Internet]. 2014;129:177–86. Available from: http://dx.doi.org/10.1016/j.apenergy.2014.04.073

27. Donkers PAJ, Pel L, Adan OCG. Experimental studies for the cyclability of salt hydrates for thermochemical heat storage. J Energy Storage [Internet]. 2016;5:25–32. Available from: http://dx.doi.org/10.1016/j.est.2015.11.005

28. Gordeeva LG, Aristov YI. Composites "salt inside porous matrix" for adsorption heat transformation: A current state-of-the-art and new trends. Int J Low-Carbon Technol. 2012;7(4):288–302.

29. Posern K. Influences of salt hydrate mixtures and pore sizes on the sorption heat of composite TES materials. Thermochim Acta. 2010;(l):1–6.

30. Posern K, Kaps C. Calorimetric studies of thermochemical heat storage materials based on mixtures of MgSO4 and MgCl2. Thermochim Acta. 2010;502(1–2):73–6.

31. Rammelberg HU, Osterland T, Priehs B, Opel O, Ruck WKL. Thermochemical heat storage materials – Performance of mixed salt hydrates. Sol Energy [Internet]. 2016;136:571–89. Available from: http://dx.doi.org/10.1016/j.solener.2016.07.016

32. Sutton RJ, Jewell E, Elvins J, Searle JR, Jones P. Characterising the discharge cycle of CaCl<inf>2</inf>and LiNO<inf>3</inf>hydrated salts within a vermiculite composite scaffold for thermochemical storage. Energy Build. 2018;162.

33. Casey SP, Aydin D, Riffat S, Elvins J. Salt impregnated desiccant matrices for "open" thermochemical energy storage - Hygrothermal cyclic behaviour and energetic analysis by physical experimentation. Energy Build [Internet]. 2015;92:128–39. Available from: http://dx.doi.org/10.1016/j.enbuild.2015.01.048

34. Casey SP, Elvins J, Riffat S, Robinson A. Salt impregnated desiccant matrices for "open" thermochemical energy storage - Selection, synthesis and characterisation of candidate materials. Energy Build [Internet]. 2014;84:412–25. Available from: http://dx.doi.org/10.1016/j.enbuild.2014.08.028

35. Gordeeva LG, Moroz EN, Rudina NA, Aristov YI. Formation of porous vermiculite structure in the course of swelling. Russ J Appl Chem. 2002;75(3):357–61.

36. Xu C, Yu Z, Xie Y, Ren Y, Ye F, Ju X. Study of the hydration behavior of zeolite-MgSO4composites for long-term heat storage. Appl Therm Eng [Internet]. 2018;129:250–9. Available from: https://doi.org/10.1016/j.applthermaleng.2017.10.031

37.   Zalba B, Marín JM, Cabeza LF, Mehling H. Review on thermal energy storage with phase change: Materials, heat transfer analysis and applications. Vol. 23, Applied Thermal Engineering. 2003. 251-283 p.

38.   Sutton RJ, Jewell E, Elvins J, SEarle JR. Characterising the discharge cycle of a thermochemical storage system involving the hydration of chemical salts . In: SETI 2016. Singapore; 2016. p. 1–10.

39.   Jenkins GJ, Perry MC, Prior MJ. The climate of the UK and recent trends [Internet]. Met Office Hadley Center. 2009. 1-122 p. Available from: http://ukclimateprojections.defra.gov.uk/images/stories/trends_pdfs/Trends.pdf

40.   Hawwash AA, Hassan H, Ahmed M, Ookawara S, Feky K El. Long-term Thermal Energy Storage Using Thermochemical Materials. Energy Procedia [Internet]. 2017;141:310–4. Available from: https://doi.org/10.1016/j.egypro.2017.11.111

41.   Aristov YI, Restuccia G, Tokarev MM, Buerger HD, Freni A. Selective water sorbents for multiple applications. 11. CaCl2 confined to expanded vermiculite. React Kinet Catal Lett. 2000;71(2):377–84.

42.   Sutton RJ, Elvins J, Casey S, Jewell E, Searle JR. The Optimsiation of Salt Impregnated Matrices as Potential Thermochemical Storage Materials . ICNTREE 2015  17th Int Conf Nucl Therm Renew Energy Eng. 2015;